Electronic States and Optical Absorption in Strained Heterostructures Under External Electric Field

G. E. Marques
Departamento de Física, Universidade Federal de São Carlos
13565-905 São Carlos, SP, Brasil

A. M. Cohen
Departamento de Física, Universidade do Amazonas
69068-900, Manaus, AM, Brasil

Received September R, 1993

We study the effects of internal strains and spatial asymmetry induced by external electric field on the electronic states, subband structure and optical absorption spectrum in II-VI semiconductor heterostructures. Excitonic effects are calculated assuming 1s hydrogenic states only. We clioose CdTe-Cd(Hg)Te and CdTe-Cd(Zn)Te as examples of heterostructures with internal strains applied inside and outside the layer where carriers are confined.

I. Introduction

Recent advances in molecular beam epitaxy for 11-VI semiconductors compounds have permitted to achieve high quality heterostructures and, therefore, produce optolectronic devices in most of the visible spectrum. The Cd(Zn)Se-CdTe-Cd(Zn)Se tiode laser is a good example of a. wide gap system working in the blue-green region, as reported recently[1-3]. Still others 11-VI compounds may work in the near- and mid-infrared region, where the effective masses for the carriers are very small, the optical nonlinearities are very large. and CdTe-Cd(Hg)Te-CdTe is a good example of material that may be used to produce efficient nem optical devices in this range.

Most of the elements in the $A^{II} - B^{VI}$ semiconductor family display zinc-blende symmetry with different lattice parameters. Therefore,lattice mismatches will induce strong internal strains in layered semiconductor systems with dramatic influences to their electronic structure. Thus, a model to obtain the electronic subbands for 11-VI heterostructures must handle this important additional contribution, in order to calculate and to reach some understanding of their optical spectra[4].

II. Optical absoiption

Optical absorption has demonstrated to he one powerful tool to reveal the nature of the electronic states in heterolayered semiconductor structures. Their experimental spectra are strongly dominated by quasi-localized excitonic transitions superimposed to plateaus due to band-to-band transitions. The plateau regions display the general aspects of the joint density of states fuiiction and the shape of the excitonic peaks gives information on Coulombic interaction between carriers and homogeneous scattering mechanisms affecting the transitions. The selection rules for optical transitions depend on the light polarization and are determined by spatial symnietry and by the strong hybridization of the electronic states involved. Interband optical transitions, wliich would be strictly "forbidden" in bulk semi-

conductors ($\Delta n = |n_f - n_i| > 0$), can easily be observed in these layered structures, although they usually display weaker intensity as compared to the "permitted" ones ($\Delta n = 0$). For example, the selection rules[5] for the optical transitions from the $n_i = n$ subband in the valence to tlie first electron subband, $n_f = 1$, becomes $\Delta n = 2p$, $p = 0, 1, 2, 3.....$ In presence of an applied electric field, F, the optical absorption coefficient for transitions froin the jth state in the valence subband, $\psi^{\sigma}_{v,j}$ $(\mathbf{F}, \mathbf{k}, \rho, z)$, to tlie i^{th} state in the conduction subband $\psi^{\sigma'}_{c,i}$ $(\mathbf{F}, \mathbf{k}, \rho, z)$, can be calculated as

$$\alpha(\hbar\omega) = \frac{\pi e^2}{L_z \ m_0 \ n_r \ \omega} \sum_{\sigma\sigma'} \int \frac{d^2k}{(2\pi)^2} \ Q^{\sigma\sigma'}_{i,j}(\mathbf{F}, \mathbf{k}) \ \mathcal{L}\{\Delta E^{\sigma,\sigma'}_{ij}(\mathbf{F}, \mathbf{k}) \ - \ \hbar\omega, \ \Gamma_{ij}\}, \tag{1}$$

in quantum wells of width L, composed of a semiconductor material with index of refraction n_r and m_0 being the free electron mass. Here, $\mathcal{L}\{x, x_0\}$ is the lineshape function for an optical transition between two states having energy difference, $\Delta E^{\sigma,\sigma'}_{ij}(\mathbf{F}, \mathbf{k})$ depending on spin components, σ, electric field strength, **F**, linear mcmentum, k, and must be calculatetl in the presence of all internal strains present in the heterostructure. The linewidths, Γ_{ij}, for these transitions are determined by all homogeneous and inhomogeneous scattering mechanisms present in tlie sample. In these strongly polar semiconductor family, coupling of carriers to LO-phonons[1] and scattering by ionized impurities are the most important contributions to the homogeneous part whereas diffusion and randomized interface imperfections, strongly dependent on each sample, are two important contributions to the inhomogeneous[1] part of the linewidth.

In the present calculation we will use a Lorentzian lineshape function for $\mathcal{L}\{x\}$, with inhomogeneous linewidth estimated from the change in the effective band gap with concentration, x, of the material as

$$\Gamma_{ij} \ = \ \frac{dE^{ij}_g}{dx} \ \{\frac{3 \ a^3_o \ (1-x) \ x}{8\pi \ a^2_{xc} \ L_z}\}, \tag{2}$$

together with the correction[6] to the volume of an exciton in tlie quantum well, V, $= 2\pi a^2_{xc}/L_z$, for quasi two-dimensional excitons[7] having effective Bohr radius a,, inside zinc-blende symmetry crystals with lattice parameter, a_0, containing 4 atoms in the fcc sublattice.

The probability for vertical optical transitions, $Q^{\sigma\sigma'}_{i,j}(\mathbf{F}, \mathrm{k})$, from the jth state in the valence subband, with "total spin" component σ, to the ith state in the conduction subband, with ((total spin" component σ', can bc calculated as a function of the projection of the linear momentum operator, **P**, in the direction of the light polarization, $\hat{\eta}$, as

$$Q^{\sigma\sigma'}_{ij}(\mathbf{F}, \mathbf{k}) \ = \ \frac{1}{m_o} \ | \ < \psi^{\sigma'}_{c,i}(\mathbf{F}, \mathbf{k}, \rho, z) \ | \ \hat{\eta}.\hat{\mathbf{P}} \ | \ \psi^{\sigma}_{v,j}(\mathbf{F}, \mathbf{k}, \rho, z) > \ |^2. \tag{3}$$

Tlie electronic states with all four z-component of total angular momentum M_z positives, labeled σ = U, are expressed in terms of tlie envelope function components in the periodic Blocli functions at the Γ-point, and ordered as $|u_1> = |\frac{1}{2}, \frac{1}{2}>$, $|u_2> = |\frac{3}{2}, \frac{3}{2}>$, $|u_3> = |\frac{3}{2}, \frac{1}{2}>$ and $|u_4> = |\frac{1}{2}, \frac{1}{2}>$, respectively for electron, heavy-hole, light-hole and split off-hole branches. For example, the spinor of four components, for a conduction band U-state in the ith electron subband is written as

$$\psi^U_{c,i}(\mathbf{F},\mathbf{k},\rho,z) = e^{i\mathbf{k}.\rho} \begin{bmatrix} F_1^{c,i}(\mathbf{F},\mathbf{k},z) \\ F_2^{c,i}(\mathbf{F},\mathbf{k},z) \\ F_3^{c,i}(\mathbf{F},\mathbf{k},z) \\ F_4^{c,i}(\mathbf{F},\mathbf{k},z) \end{bmatrix}. \quad (4)$$

The otlier set of electronic states mith all four components of total angular momentum M_z negatives, labeled a = L and degenerate with U-states in the case of symmetric potentials, are ordered in the same sequence and may be obtained from the set of U-states by the application of tlie time reversal operator, $\mathcal{T}_r = -i\,\hat{\mathcal{I}}\,\hat{C}\,\hat{\sigma}_y$, representing the spatial inversion, complex conjugation and spin flipping operators respectively. In this manner, the spinor for tlie conduction band L-state in the ith electron subband, which satisfies $\psi^L = \hat{\mathcal{T}}_r\,\psi^U$ in tlie flat-band condition, has the form

$$\psi^L_{c,i}(\mathbf{F},\mathbf{k},\rho,z) = e^{i\mathbf{k}.\rho} \begin{bmatrix} F_5^{c,i}(\mathbf{F},\mathbf{k},z) \\ F_6^{c,i}(\mathbf{F},\mathbf{k},z) \\ F_7^{c,i}(\mathbf{F},\mathbf{k},z) \\ F_8^{c,i}(\mathbf{F},\mathbf{k},z) \end{bmatrix}. \quad (5)$$

For anyone of the three other types of carriers, just replace in above expressions 'c' by 'hh', 'lh' or 'so', respectively for heavy-holes, light-holes and split off-l-ioles U- or L-states. In the next section we will present the general details of the method used to calculate these electronic states and their energy dispersions in semiconductor heterostructures and, in the following section, we will discuss effects of carrier localization, applied external field, temperature and internal strains to the these states and how they affect the optical absorption spectrum.

III. Modified k.p model

The modified Kane Hamiltonian determining each envelope function component, for U- or L-states, in a semiconductor heterostructure, as the solutions of $H^U_{\mathbf{k}.\mathbf{p}}\psi^U = E^U\,\psi^U$ for example, can be written[5] as

$$H^U_{\mathbf{k}.\mathbf{p}} = \begin{bmatrix} D_{el} & P_1 & P_2 & P_3 \\ P_1^* & D_{hh} & L_1 & L_2 \\ P_2^* & L_1^* & D_{lh} & Q_1 \\ P_3^* & L_2^* & Q_1^* & D_{so} \end{bmatrix}, \quad (6)$$

where tlie inatrix elements are given by:

$$\begin{aligned}
D_{el} &= E_g^0 + E_\nu^c + \left(F_0 + \frac{1}{2}\right) k^2 + [\hat{k}_z \left(F + \frac{1}{2}\right) \hat{k}_z]\,; \\
D_{hh} &= D^+\,;\; D_{lh} = D^-\,,\text{ where} \\
D^\pm &= -E_\nu^v - \frac{1}{2}(\gamma_1 \pm \gamma_2)\,k^2 - \frac{1}{2}[\,\hat{k}_z\,(\gamma_1 \mp 2\gamma_2)\,\hat{k}_z] \\
D_{so} &= -\Delta - [\hat{k}_z\,(\gamma_1)\,\hat{k}_z] - \gamma_1\,k^2\,; \\
P_1 &= -\sqrt{\frac{1}{2}}\,P\,k\,; \\
P_2 &= \sqrt{\frac{2}{3}}\{P,\,\hat{k}_z\} + i\sqrt{\frac{1}{6}}\,P\,k\,;
\end{aligned}$$

$$P_3 = \sqrt{\frac{1}{3}}[\ \{P, \hat{k}_z\} + i\,P\,k]\ ;$$
$$L_1 = \sqrt{3}\,k\,\{\gamma_3, \hat{k}_z\} + i\,\frac{\sqrt{3}}{2}k^2\,\gamma(\theta)\ ;$$
$$L_2 = -\sqrt{\frac{3}{2}}\,k\,\{\gamma_3, \hat{k}_z\} + i\,\sqrt{\frac{3}{2}}\,k^2\,\gamma(\theta)\ ,$$
and
$$Q_1 = \sqrt{2}\,[\hat{k}_z\,\gamma_2\,\hat{k}_z] - \frac{1}{\sqrt{2}}\,\gamma_2\,k^2 - i\,\frac{3}{2}\sqrt{2}\,k\,\{\gamma_3,\ \hat{k}_z\}$$

The symbols in tlie above expressions are: $\hat{k}_z = -i\frac{d}{dz}$; k = $\sqrt{k_x^2 + k_y^2}$; $\{\hat{A}, \hat{B}\} = (\hat{A}\hat{B} + \hat{B}\hat{A})/2$. Also, θ is tlie angle in the xy-plane defining the direction of warping in tlie valence bancl, $\gamma(\theta) = \gamma_3 - (\gamma_3 - \gamma_2)\,cos^2(2\,\theta)$; $E_\nu^v = -f\,\Delta E_g^0$ is the chemical band offset in tlie valence band ($E_\nu^c = (1-f)\Delta E_g^0$) for an interface between two inaterials defined **as** the fraction "f" of tlie band gap misalignment; E_g^0, is the unstrained gap in tlie quantum well region, and P, F_0, γ_1, γ_2 and γ_3 are the Kane-Luttinger parameters within the 8x8 **k.p** approximation and being determined directly from the experimental values of the bulk effective masses, band gap and spin-orbit energies of a given material.

The strain Hamiltonian[8,9] can be written in terms of the angular momentum operator, its components, L = $(\hat{\mathbf{L}}_x, \hat{\mathbf{L}}_y, \hat{\mathbf{L}}_z)$ and the strain tensor $\tilde{\epsilon}$ whose components are defined from the changes in the displacement vector, **u** = (u_x, u_y, u_z), of a given atom in the site of the Bravais lattice, $\epsilon_{ij} = \frac{1}{2}\left(\frac{du_i}{dx_j} + \frac{du_j}{dx_i}\right)$. First let us define the hydrostatic deformation potentials, a_h^c for tlie conduction band, a_h^v for the valence band and tlie axial deformation potentials b_u^v (biaxial) and d_u^v (spin-dependent shear deformation). Thus, the strain Hamiltonian for the conduction(c) and valence(v) states has the form

$$H_\epsilon^{c(v)} = -a_h^{c(v)}\,Tr[\tilde{\epsilon}] - 3\,b_u^v\left[\hat{\mathbf{L}}_x^2 - \frac{1}{3}\hat{\mathbf{L}}^2\right]\tilde{\epsilon}_{xx} + c.p.]$$
$$- \sqrt{2}\,d_u^v\,[(\hat{\mathbf{L}}_x\hat{\mathbf{L}}_y + \hat{\mathbf{L}}_y\hat{\mathbf{L}}_x)\tilde{\epsilon}_{xy} + c.p.]\ , \qquad (7)$$

with c.p. denoting cyclic permutation of (x,y,z) and $Tr[\tilde{\epsilon}]$ tlie trace of the tensor. Since this Hamiltonian has the same symmetry properties as the second order contribution to the **k.p** Hamiltoiiian, it can be expressed in the same set of Bloch sates at the Γ-point, tlie $|$J, M_J $>$, given above.

For heterostructures grown in the (001) direction only the terms proportional to a's and b's, in Eq.(7) will contribute to the strain Hamiltonian. Defining the strain cornponents as $\epsilon_{xx} = \epsilon_{yy} = \epsilon_\perp$ and $\epsilon_{zz} = \epsilon_\parallel$, Eq.(7) becomes

$$H_\epsilon(001) = \begin{bmatrix} \alpha_h^c & 0 & 0 & 0 \\ 0 & \alpha_h^v - \beta & 0 & 0 \\ 0 & 0 & \alpha_h^v + \beta & -\sqrt{2}\beta \\ 0 & 0 & -\sqrt{2}\beta & \alpha_h^v \end{bmatrix}. \qquad (8)$$

Here $\alpha_h^c = -2(S_{xx} + 2\,S_{xy})/(S_{xx} + S_{xy})\,\epsilon_\perp\,a_h^c$ and $\alpha_h^v = -2\,(S_{xx} + 2\,S_{xy})/(S_{xx} + S_{xy})\,\epsilon_\perp\,a_h^v$ represent the deformation energies due to the hydrostatic strain in conduction and valence bands, in terms of the elastic compliance components, S_{ij}, for the given material. It can be noticed that a hydrostatic strain changes the band gap as $E_g^* = E_g^0 + (\alpha_h^c - \alpha_h^v)$. Also, axial deformations contribute with $\beta = -(S_{xx} - S_{xy})/(S_{xx} + S_{xy})\,\epsilon_\perp\,b_u^v$ as tlie energy due to the biaxial strain, directly affecting the band offset, $\Delta E_\nu^{hh} = +\beta$ for heavy-holes and $\Delta E_\nu^{lh} = -\beta$ for the light-holes. Therefore, axial strains move heavy-hole and light-hole energy states in opposite directions and may even place light-holes above the heavy-holes, in those heterostructures' with biaxial energy, β, negative.

The overall result of the strain effect to the en-

ergy states and to the wavefunctions certainly depends if the layer is submitted to an extension or to a compression with respect to their substrate. The deformation in the xy-plane of a. heterolayerecl system is determined by the percentage of tlie lattice mismatch in the plane of the interface, $\epsilon_{\perp} = (a_{layer} - a_{sub})/a_{sub}$, where the a's stand for lattice parameter of substrate and layer respectively. Since $a_{layer} = a_{sub}(1 + \epsilon_{\perp})$, one immediately may see that under compression, $a_{layer} < a_{sub}$, the strain in the xy-plane is $\epsilon_{\perp} < 0$ and under extension, $a_{layer} > a_{sub}$, the strain in the xy-plane is $\epsilon_{\perp} > 0$.

Therefore: for an interface under strain, one must modify the band offset in order to include the hydrostatic and axial contributions to tlie chemical value as

$$\Delta E_{\nu}^{*} = \Delta E_{\nu}^{0} + \Delta E_{\nu}^{h} + \Delta E_{\nu}^{u}. \tag{9}$$

This is the proper way to take into account the different values of quantum well heights for each type of carrier. Therefore, we may also expect a change in the hybridization of tlie electronic statcs in quantum wells under strain.

VI. Quantum well subband structure in 11-VI compouds

The table below gives tlie experimental bulk parameters for two kind of heterostructures to be used in these examples, and they were taken from Refs. [11-18].

Three main difficulties are encountered in the construction of such a kind of table. The first one is an experimental value for the heavy-hole mass in the (111) direction since the number of experimental results in this direction is extremely scarcc for most of the materials. When this value is not available in the literature, we use the Luttinger parameters γ_1 and γ_3 for bulk materiais in the table of Ref. [14] and calculate the effective mass in this direction as

$$m_{hh}(111) = \gamma_1 - 2\gamma_3. \tag{10}$$

The second one resides in the determination of the hydrostatic strain parameters since only their difference is measured from the change of the hydrostatic band gap, $\Delta E_g^h = (a_h^c - a_v^h)$ although, for almost all materials, the calculated values for their ratio[18] are in the range -0.25 $\geq a_h^c/a_h^v \geq$ -0.5. The axial deformation energy, β, can be easily determined from the lifted degeneracy of light- and heavy-holes excitons, in bulk materials under strain, and the lattice parameter a(Å) is well known from X-ray diffraction, for example.

The third and last difficulty is related to the fact that CdSe has wurtzite symmetry. Therefore, the band parameters shown in the table are good for small concentrations of CdSe in Cd(Zn)Se, where we will assume that tlie lattice symmetry remains zinc-blende and, then, we may take some band parameters from bulk ZnSe.

The set of pasameters used for Cd(Zn)Se-CdTe-Cd(Zn)Se heterostructures are determined from linear interpolation between the values given in the table 1. Tlie present calculation will also assume that the samples are grown on ZnSe substrate. On the other hand, for CdTe-Cd(Hg)Te-CdTe heterostructures almost all parameters are well known and the samples will be assumed to be grown on CdTe substrate.

The experimental band gap for Cd(Hg)Te, measured in meV, a.s determined from the best fit to[18] optical data as a function of temperature, T, and concentration, x, is given by

$$E_g(x,T) = -313 + 1787x + 444x^2 - 1237x^3 + 932x^4 + (667 - 1714x + 760x^2)\frac{T}{1000}. \tag{11}$$

The details to obtain the modified Kane Hamiltonian, the eigen-energies and eigen-states of the problem

Parameter	CdTe	HgTe	ZnSe	CdSe
m_{el}	0.096	0.031	0.147	0.130
$m_{hh}(001)$	0.410	0.420	0.780	0.780
$m_{lh}(001)$	0.103	0.026	0.149	0.149
$m_{so}(001)$	0.280	0.102	0.300	0.300
$m_{hh}(111)$	0.530	0.530	0.304	0.3040
E_g^0 (meV)	(eq.11)	(eq.11)	2820	1840
Δ (meV)	930	1080	430	420
a_h^c (meV)	-2560	-2370	-4157.1	-2142.9
a_h^v (meV)	1280.0	900.0	1662.9	857.2
b^v (meV)	-1150	-1150	-1200	-1800
d^v (meV)	-1150	-1150	-3800	-2700
a (Å)	6.4810	6.4610	6.481	6.461
C_{11} (10^2 kbar)	5.660	5.971	7.890	5.971
C_{12} (10^2 kbar)	3.960	4.154	4.980	4.154
C_{44} (10^2 kbar)	2.070	2.259	2.070	2.259

Table 1: Experimental values which determine Kane parameters used in present work

$$[\,H_{\mathbf{k}.\mathbf{p}} + H_{\epsilon}(001) + H_{field}\,]^{U(L)}\ \psi_{i,j}^{U(L)}(\mathbf{F},\mathbf{k},\rho,z) = E_{ij}^{U(L)}(\mathbf{F},\mathbf{k})\ \psi_{i,j}^{U(L)}(\mathbf{F},\mathbf{k},\rho,z), \tag{12}$$

was discussed in Refs. [5] and [20]. Here we will present effects due to hybriclization (subband mixing) of these eigen-states and the internal strain built into the layers on tlie optical absorption, by analyzing the dependeiice of the envelope function components $F_{j,n}^{i,m}(\mathbf{F},\mathrm{k},z)$ on both the linear momentum k and internal strains determined from interfacial lattice mismatch with respect to a chosen substrate.

At the zone center, k=0, the mixing of states depends more stiongly on the axial cleformation potential, b_u^v. We choosr to keep the assignment foi the character of each valence envelope function 2 to 4 or 6 to 8 above, as associated to tlieir origin in the unstrained bulk states and usually labeled lieavy-hole (HH), light-hole (LH) and split-off (SO). We also adopt to label a transition from tlie valence to the conduction subbands, such as HH, — $EL_{n'}$, as simply tlieir initial electronic state in the valence subbands $HH_{nn'}$, $LH_{nn'}$ or $SO_{nn'}$ where, for U-states(L-states) the total angular moinentum component at the zone center, are $M_J = +(-)\frac{3}{2}$, $M_J = +(-)\frac{1}{2}$, and $M_J = +(-)\frac{1}{2}$, respectively. The hybridization of these states can be deteriniied by calculating the average of the z-component of total angular momentum, $< J_z > (\mathbf{k}) = \sqrt{< \hat{J}_z^2 >}$ as a function of the linear momentum k.

Part (a) of Fig. 1 shows the calculated hybridization, within the present model, for three heavy-holes and two light-holes in $Cd_{0.85}Hg_{0.15}Te - Cd_{0.27}Hg_{0.73}Te - Cd_{0.85}Hg_{0.15}Te$ quantum well with L, = 50 h, for temperature T = 80 K and an applied electric field, F = 2.0 kV/cm. The valence chemical band offset [16] for these II-VI family of heterostructures are in the range between 20.0 meV < E_ν^v < 100.0 meV.

Since we have assumed that the substrate is CdTe, therefore, we find internal strains applied both to the harrier and to the well layers. The temperature affects the valence subband mixing, since it decreases the

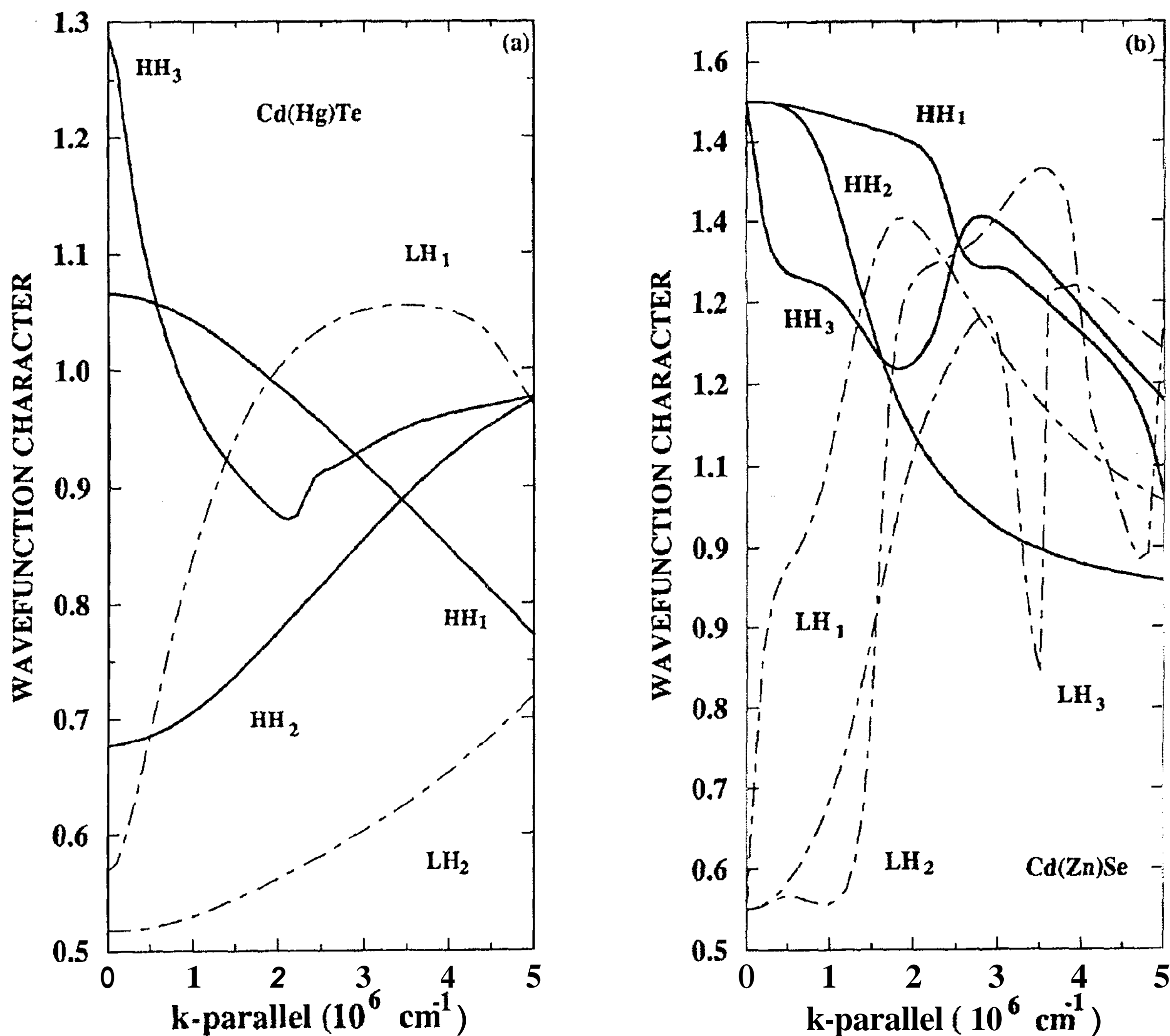

Figure 1. Excliaiige of cliaracter between electronic states in tlie valence subband of a 11-VI quantum well, as a function of tlie linear momentum, within tlie full k.p scheme. Part (a) shows the liybridization in $Cd_{0.85}Hg_{0.15}Te$ − $Cd_{0.27}Hg_{0.73}Te$ − $Cd_{0.85}Hg_{0.15}Te$ quantum well, with L, = 50 Å, at ternperature T = 80 K under applied electric field F = 2.0 kV/cm. Part (b) shows the Iiybridization in $Cd_{0.25}Zn_{0.75}Se$ − $ZnSe$ − $Cd_{0.25}Zn_{0.75}Se$ quantum well, with L, = 200 Å, at temperature T = 0 K, under applied electric field F = 2.0 kV/cm.

band gap and, therefore, we expect an increase in tlie conduction-valence band coupling. The most dramatic contribution for this material, however, comes from the biaxial strain that causes an increase in the barrier heiglit for heavy-holes and a decrease for tlie light-lioles. This change already breaks the degeneracy at $k = 0$, affecting tlie admixture of valence states. In tlie present quantum well in part (a), there are two heavy-holes and one light-hole state bound to the well and the other two are just in the continuum. As k-parallel increases, the states exchange their characters but remain with a value for the cornponent of total angular momentum near the average value 1.0. Notice also that the nearly free states, HH_3 and LH_2, approach their bulk value for the total angular momentum, only close to k = 0.

In tlie right side of Fig. 1, part (b), we have shown another example of hybridization of valence subbands in a material where tlie internal strains are applied only to the barrier layer, since tlie substrate, for this sample, was assumed to be ZnSe. The well width here is 200 Å, the temperature is T = 0 K and the applied electric field F = 2.0 kV/cm. The valence levels appear ordered sequentially, as HH_n, LH_n, HH_{n+1}, LH_{n+1}, and we find three heavy-holes and two light-holes inside this well. The exchange of character is very pronounced

since the levels are close in energy due to the large value of well width, what enhances their admixture. These effects would affect strongly the optical absorption spectrum, via the dependence of the transition probability Q's, in eq.(3), and, consequently, the intensity of each peak via their oscillator strengths. For less mixture in the states, the optical absorption and their selection rules tend to appear more likely as in bulk optical transitions.

The character of SO_n and EL_n states, not shown in fig.(1), also deviate from their bulk values, 0.5, as k-parallel increases. Therefore, it is a direct consequence of this complex hybridization process that the conduction subbands display their well known strong nonparabolicity. It should be also noticed that these changes in the wavefunction characters from their bulk values decrease for increasing subband number since higher states should appear more like bulk states.

Finally, the last effect which produces changes in the subband mixing is the inclusion of the split-off branch. In general, internal strains affect SO_n states in the same manner as for the light-holes, since there is a strong interaction only between these two branches, as can be inferred from the Hamiltonians in Eq.(7) and Eq.(8). In general, the spin-orbit will push light-hole states upwards and, therefore, also influencing the interaction between light and heavy holes.

The applied field has a much stronger effect on the mixing since it also tends to decrease the effective gap and, more important of all, lifts the degeneracy between L-states and U-states at $k \neq 0$. As an example of this effect, we show in the left side of fig.2, the first two conduction subbands dispersions for both U- and L-states, in $Cd_{0.85}Hg_{0.15}Te - Cd_{0.27}Hg_{0.73}Te - Cd_{0.85}Hg_{0.15}Te$, with well width, L, $= 80$ Å, at temperature $T = 80\ K$ and under an applied electric field, $\mathbf{F} = 15\ kV/cm$. One may easily observe the strong nonparabolicity, present in our modified **k.p** Hamiltonian and induced by the spatial localization of electrons in the well region. Notice that the spin splitting in the conduction band is smaller than in the valence subbands since electron states are found in a deeper quantum well. Due to the large scale of energy in the conduction subbands, we are including an inset where we see that typical values for the electron spin splitting may be as large as 1.8 meV, which compares very well with experimental results for GaAs quantum wells, reported in Ref. [19].

In part (b), we show the valence subband dispersions and their stronger spin splitting produced by the field. Notice also, that the states closer to the border are more affected due to their larger probability to tunnel out the quantum well region, thus changing the spatial form of the wavefunction from "localized" to "resonant". It is also apparent that the changes induced by the electric field in the subband admixture, close to the minigap regions, will affect the effective masses and also the oscillator strengths, since the electric field pushes electrons and holes in opposite directions.

In part (a) of Fig. 3 we show the first two electronic dispersions, for U-states only, in the same Cd(Hg)Te quantum well, as described in Fig. 1. Although difficult to observe from the figure, each subband displays a different curvature. The effective masses for the first three electron states in Cd(Hg)Te and calculated at the $k = 0$, are 0.00938 (0.01071) m_0, 0.01021 (0.09309) m_0 and 0.01644 (0.018542) m_0 respectively without (with) the applied electric field ($\mathbf{F} = 2.0\ kV/cm$) and, for the sake of comparison, their bulk values, as interpolated from Table 1, are $m_{el} = 0.01812\ m_0$ in the well and $m_{el} = 0.10488\ m_0$ in the barrier regions. It becomes apparent that the spatial localization of carriers in the quantum well region tends to decrease the in-plane effective masses at first, however they must approach the, barrier (well) value as the subband index and/or the k-parallel increase or the well width decreases (increases). Notice, furthermore, an almost linear shift in the energy subband dispersions caused by the temperature, as can be observed from dotted and solid curves in the figure. The inset, in part (a), shows qualitatively that

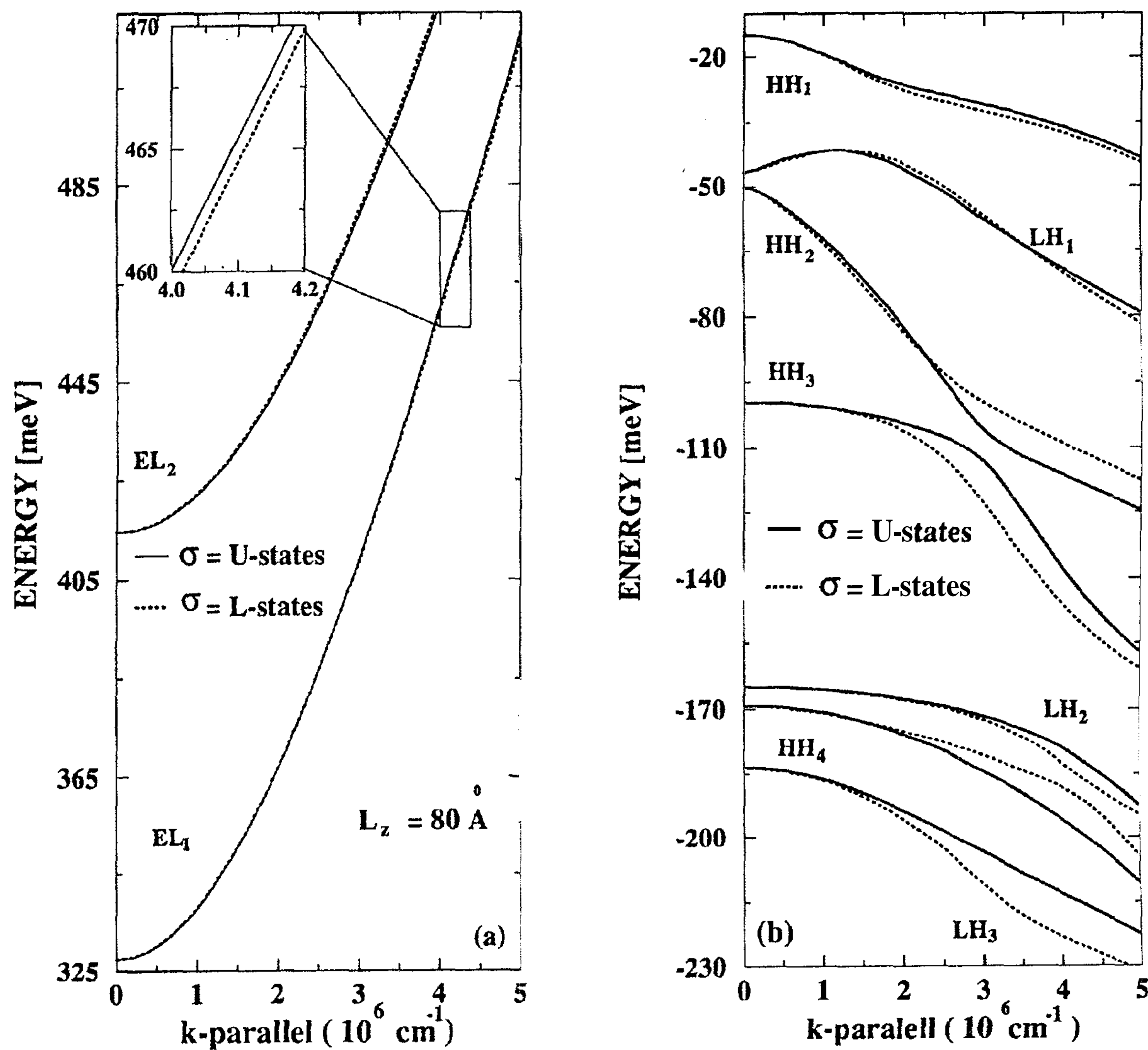

Figure 2. The spin splitting of all carriers induced by tlie spatial asymrnetry due to tlie external electric field, in $Cd_{0.85}Hg_{0.15}Te$ − $Cd_{0.27}Hg_{0.73}Te$− $Cd_{0.85}Hg_{0.15}Te$ quantum well, with L_z = 80 Å, at temperature T = 80 K under applied electric field F = 15.0 kV/cm.

tlie change in the effective band gap, as induced by tlie applied electric field, is similar to the effect due to temperature which, however, lias an opposite effect on the effective masses of carriers, sincc temperature changes the Kane parameters.

For Cd(Zn)Se quantum well, in part (c) of fig.3, thc effective masses for the first three localized electrons are 0.3307 (0.2205) m_0, 0.1436 (0.1454) m_0 and 0.220 (0.15611) m_0 respectively without (with) the applied field and, for the sake of comparison, their interpolated bulk valucs, from the Tablc 1, are 0.14275 m_0 in the well and 0.14700 m_0 in the barrier, respectively.

In this wide quantum well, one more effect related to tlie spatial localization of carriers may also be observed, when tlie energy of a nearly free state, EL_3, approaches the value of a bound state, EL_2. The strong nonparabolicity observed between these branches, close to k = 2.5 10^6 cm^{-1}, is due to a combination of the following effects: i) a curvature of each branch is composed of a mixture of the well and barrier masses, as present. in the boundary conditions connecting both the wave functions and their derivatives, ii) this curvature is modified by tlie spatial localization of carriers in the potential well region and iii) coupling between states, present in the **k**.**p** method. Therefore, electronic states "above the barrier region" (free states) must display

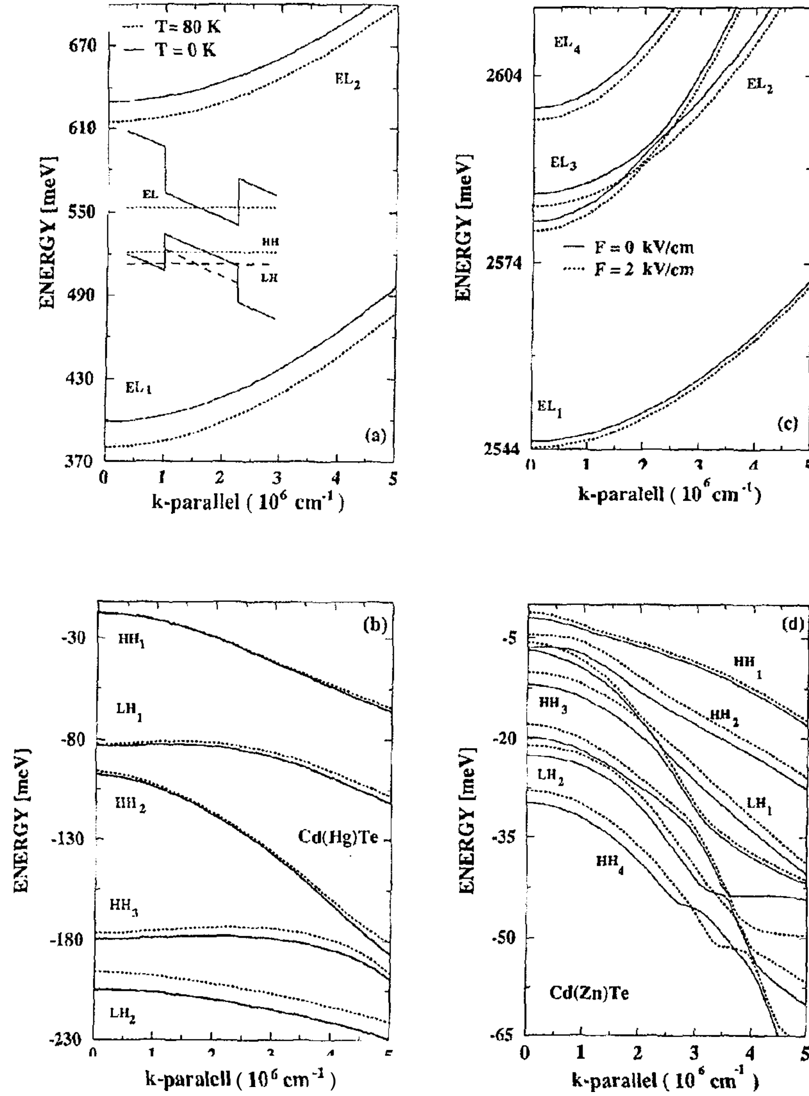

Figure 3. On tlie *left* we show the subband dispersioiis in $Cd_{0.85}Hg_{0.15}Te$ – $Cd_{0.27}Hg_{0.73}Te$ – $Cd_{0.85}Hg_{0.15}Te$ quantum well, with L, = 50 Å, at temperatures T = 80 K and T = 0 K, under applied electric field F = 2.0 kV/cm. *The* top (bottom) part shows the conductioii (valence) subbands. On tlre right we show subband dispersions for $Cd_{0.25}Zn_{0.75}Se$ – $ZnSe$ – $Cd_{0.25}Zn_{0.75}Se$ quantum well, with L_z = 200 Å, at temperature T = 0 K, under applied electric field F = 2.0 kV/cm and F = 0.0 kV/cm. The top (bottom) part shows the conduction (valence) subbands.

effective masses much closer to the bulk values of tlie materials in the barrier.

In tlie valence subbands of both materials in part (b) and (d) of Fig. 3, the overall shape of tlie dispersions are similar to typical subbands in the well known GaAs-Ga(Al)As heterostructures. It is interesting, however, to give here the values foi the effective masses at k = 0 since they will determine the binding energy of excitons and, therefore, affect the optical absorption spectrum for the quantum well.

In the Cd(Hg)Te quantum well in part (b), the top four valence subband dispersions have effective masses -0.112 (-0.112) m_0, $0.167 ($0.175) m_0, -0.05437 (-0.05397)m_0 and +0.238 (+0.000)m_0 respectively with (witliout) the applied electric field.

In the Cd(Zn)Se yuantum well, the top four valence subband dispersions have effective masses -0.162 (-0.158) m_0, +0.0993 (-0.531) m_0,-0.0518 (-0.136)m_0 and -0.197 (-0.2051)m_0 respectively with (without) the applied electric field. One should notice the important role played by the electric field on the dispersion and on the sign of the curvatures of light-hole states. The fact that the curvature of a light-hole is positive (electron-like) at k = 0 makes a difference in the calculation

of binding energies of liglit-liole excitons. In fact, it determines the minimum area of tlie k-space which is necessary to take into account, in a proper calculation of the binding energies of light-liole excitons.

The Coulombic interaction for electron-hole pairs produces a shift in the optical absorption spectrum (binding energy) and a very large increase in tlie intensity of excitonic peaks present in those spectra. In this work, tlie binding energy for excitons is calculated, as described in Ref.[5], from the effective masses obtained from tlie subband dispersions of each carrier.

In tlie left side of fig.(4) we show the calculated optical absorption spcctra for the quantum well, $Cd_{0.85}Hg_{0.15}Te - Cd_{0.27}Hg_{0.73}Te - Cd_{0.85}Hg_{0.15}Te$ with $L,$ = 50 Å under applied field F = 2.0 kV/cm and for two values of temperature, T = 80 K and T = 0 K. As an example of the effect of the Coulombic interaction contrihution it is also shown, in dot-dashed line, the optical absorption calculated without tlie contribution froin the excitons. Notice the resemblance of a normal steplike stair for a typical joint density of states of a two-dimensional electron gas. Here tlie nonparabolicity of conduction subbands, tlie abnormal dispersions of tlie valence subbands and the linewidth for band-to-band optical transitions are responsible for the changes in the joint density of states between two steps and the overall shape of the spectral line without excitons.

In the right side of Fig. (4) we show tlie calculated optical absorption spectrum for the quantum well, $Cd_{0.25}Zn_{0.75}Se - ZnSe - Cd_{0.25}Zn_{0.75}Se$ with $L,$ = 200 Å under applied electric field F = 2.0 kV/cm and for temperature T = 0 K. The strong mixing in the valence subbands and small values for tlie optical linewidths inakes possible to see both band-to-baiid and excitonic optical transitions. The broader optical absorption spectrurn was calculated without (daslied line) and with (dot-dashed line) excitoiiic effect for 6.0 meV of inhomogeneous linewidths for both types of transitions. Inhomogeneous linewidths associated with possible scattering mechanisms may give a good indication on the quality of the sample. The solid line shows an optical absorption for a good sample witli both excitonic and band-to-band linewidths having small values, tlierefore both transitions may be observed. The difference in tlie intensities of peaks are related to the change in their oscillator strengths, as induced by spatial symmetry for two states calculated in tlie **k**.**p** scheme.

V. Summary

To summarize, we have presented in this communication aspects of a powerful calculational model, based oii tlie full Kane-Luttinger k p Hamiltonian, and used it to determine electronic structure of 11-VI semiconductor heterostructures under the action of external and internal fields for different values of temperature. We Iiave also discussed some intrinsic details of Kramers degeneracy of these electronic states and its breakdown under spatially asymmetric potentials, their effects on the subband dispersions, effective masses of localized carriers and the hybridization of the valence band states. Finally, we have shown general aspects of tlie calculated optical ahsorption spectrum for different scattering mechanisms. We Iiave concluded that the overall shape of the optical spectrum may give importaiit informations on the quality of a sample and, possibly, distinguish on the dominant mechanism of scattering determining the linewidths for the optical transitions in tlie sample.

Acknowledgements

Authors acknowledge partial financial support from Conselho Nacional de Desenvolvimento Científico e Tecnológico - CNPq.

References

1. N. T. Pelekanos, J. Ding, M. Hagerott, A. V. Nurmikko, H. Luo, N. Samarth and J. K. Furdyna, Phys. Rev. B**45**, 6037 (1992).

2. D. Ahn, T. K. Yoo and H. Y. Lee, Appl. Phys. Lett. 59, 2669 (1991).
3. M. A. Haase, J. Qiu, J. M. DePuydt and H. Cheng, Appl. Phys. Lett. 59, 1272 (1991)
4. D. Chemla, S. Schmitt-Rink and D. A. B. Miller, in *Optical Nonlinearities and Instabilities in Semiconductors*, edited by *H.* Haug (Academic, New York, 1978), p.83.
5. A. M. Cohen, and G. E. Marques, Phys. Rev. B41, 10603 (1990).
6. K. H. Goetz, D. Bimberg, H. Jürgensen, J. Selders, A. V. Solomonov, G. F. Glinskii, and M. Razeghi, J. Appl. Phys. 54, 4543 (1983).
7. J. Hegarty, and M. D. Sturge, J. Opt. Soc. Am. 2, 1143 (1985).
8. G. L. Bir aiid G. E. Pikus, *Symmetry and Strain-Induced Effects in Semiconductors* (Wiley, N.Y. 1974).
9. M. Chandrasekhar and F. H. Pollack, Phys. Rev. **B15**, 2127 (1977).
10. *Physics and Chemistry of II-VI compounds*, edited by *M.* Aven and J. P. Prener (North Holland, Amsterdam, 1976)
11. A. Blacha, H. Presting and M. Cardona.. Pliys. Stat. Sol. (b) 126, 11 (1984).
12. *Numerical* Data *and Functional Relationships in Sciençes and Technology*, edited by *O.* Madelung, Landolt-Bornstein-New Series, Group III, vol.17b (Springer, Berlin, 1982).
13. R. Dornhaus and G. Nimtz in *Springer Tracts in Modern Physics 78,* edited by G. Hohler (Springer, Berlin, 1976).
14. P. Lawaetz, Phys. Rev. B4, 3460 (1971).
15. C. G. van de Walle, Phys. Rev. B**39**, 1871 (1989).
16. *Properties of Mercury Cadmium Telluride, EMIS Datareviews series* No. 3, edited by J. Brice and P. Caper (INSPEC - Institute of Electrical Engineers, Survey, England, 1987)
17. D.L.Camphausen, G. A. N. Connell and W. Paul, Phys. Rev. Lett. **26,** 184 (1971).
18. M. Murayama and T. Nakayama, Proc. 6th Int. Conf. on Superlattices, Microstructures and Microdevices (Xi'an, China, 1992).
19. B. Jusserand, D. Richards, H. Peric and B. Etienne, Phys. Rev. Lett. 69, 848 (1992)
20 A. M. Cohen, S. R. Aladim and G. E. Marques, Surf. Sci. 267, 464 (1992).